High Resolution Study of the Rotational Spectrum of Formaldoxime, Combined with Quantum Chemical Calculations, Its ^{14}N Spin-Rotation Coupling, ^{14}N Nuclear Quadrupole hfs, and Its Rotational Zeeman-Effect

A. Klesing and D. H. Sutter

Abteilung Chemische Physik im Institut für Physikalische Chemie der Christian-Albrechts-Universität zu Kiel, Kiel, Germany

Z. Naturforsch. **45a**, 817–826 (1990); received April 2, 1990

A high resolution study of the rotational spectrum of formaldoxime was carried out with the aim to resolve a discrepancy between early microwave results and recent ab initio calculations. Accurate ^{14}N quadrupole coupling constants and spin-rotation coupling constants could be derived from zero field hfs multiplets. From the Zeeman-splittings in external magnetic fields up to 18 kGauss the diagonal elements of the molecular g-tensor and the anisotropies in the diagonal elements of the molecular magnetic susceptibility tensor were obtained and were used to derive the diagonal elements of the molecular electric quadrupole moment tensor. For comparison, Hartree Fock SCF calculations were carried out with a basis of TZVP quality. As it turned out such calculations are able to reproduce the molecular electric quadrupole moment tensor but fail to reproduce the ^{14}N nuclear qudrupole coupling constants to better than 0.3 MHz. A revised formula to predict spin-rotation coupling constants of first row elements such as nitrogen is also proposed.

Introduction

The microwave spectrum of formaldoxime, $H_2C=NOH$, was studied first by Levine [1–3] and independently by Pillai [4]. These studies lead to the complete substitution structure (r_s-structure) shown in Figure 1. They also lead to moderately accurate experimental values for the electric dipole moment [1] and for the nitrogen quadrupole coupling tensor. Later this original work was complemented by Kaushik and Tagaki [5] who presented a centrifugal distortion analysis and distortion corrected rotational constants. Recently Palmer [6] has presented SCF ab initio results of TZVP quality (triple zeta valence plus polarization) for the quadrupole coupling constants which deviated from the early microwave results. In the meantime Gerber and Huber [7] have presented evidence that present-day ab initio methods quite in general have difficulties in calculating the electric field gradients at sp^2-hybridized nitrogen nuclei.

In the following we report the results of a high resolution microwave Fourier transform study which also includes the investigation of the molecular rotational Zeeman-effect. From this study we are now able to present molecular quadrupole coupling constants with considerably reduced experimental uncertainties for better comparison with ab initio results. The high resolution which could be achieved made it possible to determine also the ^{14}N spin-rotation coupling constants for the first time. Furthermore, from the high-field rotational Zeeman-effect splittings, experimental values could be determined for the diagonal elements of the molecular magnetic g-tensor and for the anisotropies in the molecular magnetic susceptibility tensor. These Zeeman data could be used to derive the

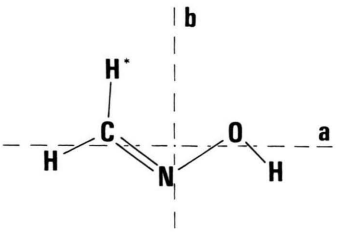

Fig. 1. Complete r_s-structure of formaldoxime taken from [3]. It is used as input for the quantum chemical calculations and for the derivation of the anisotropies in the second moments of the electron coordinates.

Bond lengths (Å)				Interatomic angles	
	C		O	H*–C–N	121.77°
N	1.276	N	1.408	H–C–N	115.55°
H	1.086	H	0.956	C–N–O	110.20°
H*	1.085			N–O–H	102.68°

Reprint requests to Prof. Dr. D. H. Sutter, Institut für Physikalische Chemie, Universität Kiel, Olshausenstr. 40–60, D-2300 Kiel 1.

0932-0784 / 90 / 0600-0817 $ 01.30/0. – Please order a reprint rather than making your own copy.

diagonal elements of the molecular electric quadrupole moment tensor and the anisotropies in the second moments of the electronic charge distribution.

Parallel to the experiments, Hartree Fock SCF calculations were carried out. Combining the experimental data with our new ab initio value for the out-of-plane second electronic moment, $\langle c^2 \rangle$, we can also predict a fairly accurate value for the hitherto unknown magnetic bulk susceptibility. Finally the nitrogen spin-rotation coupling constants, the nuclear quadrupole coupling constants, and the molecular electric quadrupole moments are discussed in comparison to quantum chemical results.

Experimental

Formaldoxime was prepared from formaldehyde and hydroxylamine hydrochloride as described in [8]. The sample, a white powder, was sublimized at room temperature into the brass waveguide absorption cells. The cells themselves were cooled by methanol circulating at a temperature of $-60\,^{\circ}C$ in a cooling jacket attached to the absorption cells. Sample pressures were kept close to 1 mTorr. Since the quality of the signals slowly degraded, the cells were evacuated and refilled after about one hour of measuring time.

The spectra were recorded with our new Fourier transform spectrometer described in [9, 10]. Under the conditions mentioned above, typical effective relaxation times, T_2, were on the order of 7 μsec. This corresponds to full widths at half height of 23 kHz in standard CW absorption spectroscopy. Both μ_a- and μ_b-type transitions were investigated. Since, for closely spaced lines, the standard discrete Fourier transform technique leads to comparatively large deviations of the peaks of the power spectra with respect to the true resonance frequency [11–13], the observed transient molecular signals were analysed in a two step procedure. First indeed a discrete Fourier transform analysis was carried out, but this analysis only provided the initial values for a subsequent nonlinear iterative least squares fit of the frequencies, amplitudes, phases, and decay times directly to the observed decays [14].

For the Zeeman studies, the absorption cells were located between the pole faces of a powerful electromagnet with a gap length of 2.5 m. (For details compare Chapt. 3A of [15].) The magnetic field was recorded with a Rawson Lush 920M rotating coil gaussmeter calibrated to better than 1 Gauss against an NMR probe. The experimental uncertainty in the magnetic field was determined by the long time stability of the current stabilized power supply of the electromagnet. However, over a period of 1 hour the field fluctuations at the center of the gap never exceeded 5 Gauss. To give an impression of the quality of the spectra obtained in the present investigation we present a zero-field and a high-field Zeeman spectrum in Figs. 2 and 3, respectively.

Analysis of the Observed hfs- and Zeeman-hfs Multiplets

The zero-field ^{14}N hfs multiplets of a total of 12 low-J rotational transitions, 7 of a-type and 5 of b-type,

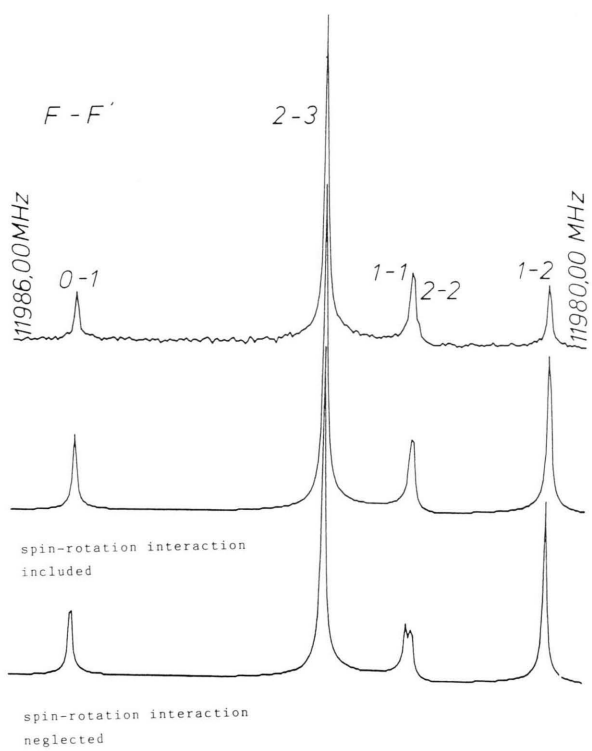

Fig. 2. Amplitude spectrum of the transition $1_{11} \rightarrow 2_{02}$. The significance of spin-rotation coupling is emphasized in the calculated spectra below the experimental pattern: These two traces show Fourier transform amplitude spectra calculated from decays simulated within the short-pulse-plane-wave approximation for the polarizing microwave [33]. The experimental delay time (0.65 μsec) between the end of the polarizing pulse and the start of sampling was also used in the simulations. Under neglect of spin-rotation interaction the transitions $F \rightarrow F' = 1 \rightarrow 1$ and $2 \rightarrow 2$ would clearly split.

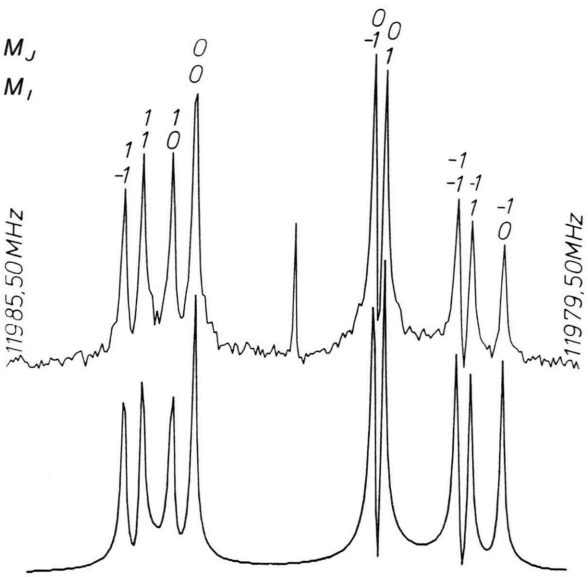

Fig. 3. Amplitude spectrum of the transition $1_{11} \rightarrow 2_{02}$ under selection rule $\Delta M_J = 0$ (and $\Delta M_I = 0$) at 10494 Gauss. The trace below shows the corresponding calculated multiplet (compare Figure 2). The "satellite" without quantum numbers is a coherent perturbation at the polarisation frequency and does not belong to the multiplet.

B_a	67 679.209(6)
B_b	11 859.127(6)
B_c	10 080.185(9)
$\chi_+ = \chi_{bb} + \chi_{cc}$	−3.0002(32)
$\chi_- = \chi_{bb} - \chi_{cc}$	−6.3799(24)
$\chi_{aa} = -\chi_+$	3.0002(32)
$\chi_{bb} = (\chi_+ + \chi_-)/2$	−4.6900(20)
$\chi_{cc} = (\chi_+ - \chi_-)/2$	1.6898(20)
M_{aa}	−0.0222(18)
M_{bb}	−0.0028(5)
M_{cc}	−0.0015(5)

Table 1. Rotational constants [5], our ^{14}N quadrupole coupling constants and our spin-rotation coupling constants [MHz] of formaldoxime. Numbers in parentheses are one standard deviation in units of the least significant figure.

Table 2. Correlation coefficient matrix of the least squares fit.

	χ_+	χ_-	M_{aa}	M_{bb}	M_{cc}
χ_+	1.000				
χ_-	−0.270	1.000			
M_{aa}	0.173	0.004	1.000		
M_{bb}	−0.024	0.014	0.778	1.000	
M_{cc}	−0.066	0.079	0.677	0.890	1.000

were recorded. They were analysed within the standard rigid rotor approximation taking into account the ^{14}N nuclear quadrupole interaction and the ^{14}N spin-rotation interaction (see (2) and (3) of [16] and references cited therein).

In Table 1 we list the ^{14}N quadrupole constants and the spin-rotation coupling constants for formaldoxime. They were obtained from an iterative least squares fit to the observed hfs multiplets (see Table 3). Also given are the rotational constants [5], since they enter into the fit via the angular momentum expectation values. In Table 2 we give the correlation coefficient matrix of this fit. The hfs splittings listed in Table 3 are given with respect to the hypothetical center frequencies of the multiplets [17]. Also given in this Table are the relative intensities of the satellites as they would be observed in a standard CW spectrometer.

For the analysis of the Zeeman-hfs multiplets the zero field Hamiltonian was supplemented by the first and second order Zeeman-effect [15] and the nuclear Zeeman-effect of the nitrogen nucleus as described by (6) through (9) of [16]. The nitrogen g-value, $v = 0.4036$, and the values for the fundamental constants were taken from the appendices E and D of [18]. ^{14}N nuclear shielding, or better its anisotropy, was neglected.

Our observed Zeeman-hfs splittings are presented in Table 4. Since the magnetic field effectively uncouples spin and overall rotation (compare [15] and Fig. 5 of [19]), the quantum numbers of the limiting uncoupled basis $|I, M_I\rangle |J, K_a, K_c, M_J\rangle$ are used in this Table to designate the states. Here M_I and M_J represent the projection quantum numbers of the ^{14}N spin, $\boldsymbol{I}$, and of the overall rotational angular momentum, $\hbar \boldsymbol{J}$, on the magnetic field axis. Note that if the uncoupling were really complete, i.e. if the influence of the matrix elements off-diagonal in the quantum numbers M_J and M_I were negligible, the M_J, $\pm M_I$ satellites in Fig. 3 should be superimposed (compare (7) of [16]). With the high resolution achieved in time domain spectroscopy they still show up as clearly separated doublets. As in Table 3, the splittings are given with respect to the hypothetical center frequency of the transition. In Table 5 we present our optimized molecular g-values and molecular magnetic susceptibility anisotropies. They were fitted to the observed splittings as described in [20]. Due to the presence of the quadrupole nucleus, the sign of the g-values could be determined from intermediate field multiplets [15, 19]. The opposite choice of signs could also be discarded for a second reason. It would lead to a negative value for the out-of-plane second electronic moment $\langle c^2 \rangle$, which is clearly impossible. In Table 6 we give the correlation coefficient matrix of the fit. We note that even with an apparently large correlation coefficient of 0.971, g_{bb} and g_{cc} are still well determined.

Table 3. Measured transition frequencies used for fitting the nuclear quadrupole coupling constants and the spin-rotation coupling constants of formaldoxime. Also given are the calculated and observed frequency splittings with respect to the hypothetical center frequency and the relative intensities which would be observed in a standard CW absorption spectrometer.

$J_{K_a K_c} \rightarrow J'_{K'_a K'_c}$	F	F'	$\nu_{obs.}$	$\Delta\nu_{obs.}$	$\Delta\nu_{calc.}$	$\delta\nu$	rel. int./%
$\nu_{central}$: 21 939.3118(5) MHz							
1 0 1 → 0 0 0	0	1	21 937.818	−1.501	−1.505	0.004	20.00
	1	1	21 940.059	0.747	0.748	−0.001	60.00
	2	1	21 939.164	−0.148	−0.148	0.000	100.00
$\nu_{central}$: 11 982.2729(2) MHz							
1 1 1 → 2 0 2	1	1	11 981.818	−0.455	−0.453	−0.002	17.86
	2	2	11 981.797	−0.476	−0.476	0.001	17.86
	0	1	11 985.326	3.053	3.053	0.000	23.81
	1	2	11 980.366	−1.907	−1.907	−0.000	53.57
	2	3	11 982.722	0.449	0.449	0.000	100.00
$\nu_{central}$: 5337.1626(13) MHz							
2 1 1 → 2 1 2	1	2	5 336.406	−0.757	−0.762	0.006	12.05
	2	1	5 337.919	0.756	0.760	−0.003	12.05
	2	3	5 338.193	1.030	1.035	−0.005	12.50
	3	2	5 337.264	0.101	0.104	−0.003	12.50
	1	1	5 335.572	−1.591	−1.597	0.006	36.16
	2	2	5 338.752	1.589	1.594	−0.005	55.80
	3	3	5 336.709	−0.454	−0.454	0.001	100.00
$\nu_{central}$: 11 568.0487(4) MHz							
3 0 3 → 2 1 2	2	2	11 567.924	−0.125	−0.130	0.005	8.64
	3	3	11 568.603	0.554	0.554	0.000	8.64
	2	1	11 567.083	−0.966	−0.965	−0.001	46.67
	3	2	11 569.162	1.113	1.112	0.001	69.14
	3	4	11 567.695	−0.354	−0.354	−0.000	100.00
$\nu_{central}$: 10 673.4421(6) MHz							
3 1 2 → 3 1 3	2	3	10 672.596	−0.846	−0.852	0.006	6.58
	3	2	10 674.604	1.162	1.168	−0.006	6.58
	3	4	10 674.698	1.256	1.256	−0.000	6.67
	4	3	10 673.252	−0.190	−0.192	0.002	6.67
	2	2	10 672.162	−1.280	−1.278	−0.002	52.67
	3	3	10 675.038	1.596	1.594	0.002	69.71
	4	4	10 672.912	−0.530	−0.529	−0.001	100.00
$\nu_{central}$: 35 783.0786(7) MHz							
4 0 4 → 3 1 3	4	4	35 783.634	0.555	0.543	0.012	5.11
	3	2	35 782.431	−0.648	−0.646	−0.002	58.44
	4	3	35 783.959	0.880	0.880	−0.000	76.70
	5	4	35 782.765	−0.314	−0.315	0.001	100.00
$\nu_{central}$: 26 665.8831(7) MHz							
5 1 4 → 5 1 5	5	5	26 667.476	1.593	1.591	0.002	68.36
	4	4	26 664.817	−1.066	−1.065	−0.001	81.33
	6	6	26 665.274	−0.609	−0.609	0.000	100.00
$\nu_{central}$: 7 424.4979(14) MHz							
7 1 6 → 6 2 5	6	5	7 423.949	−0.549	−0.547	−0.002	74.66
	7	6	7 425.418	0.920	0.917	0.003	86.43
	8	7	7 424.109	−0.389	−0.388	−0.001	100.00
$\nu_{central}$: 5 163.2016(9) MHz							
7 2 5 → 7 2 6	6	6	5 162.997	−0.205	−0.202	−0.002	74.66
	7	7	5 163.530	0.328	0.327	0.001	86.43
	8	8	5 136.068	−0.134	−0.134	0.000	100.00
$\nu_{central}$: 35 878.4857(3) MHz							
8 1 7 → 7 2 6	7	6	35 877.984	−0.502	−0.501	−0.001	77.54
	8	7	35 879.343	0.857	0.856	0.001	88.08
	9	8	35 878.117	−0.369	−0.369	0.000	100.00
$\nu_{central}$: 8 493.9651(3)							
8 2 6 → 8 2 7	7	7	8 493.715	−0.250	−0.250	−0.000	78.69
	8	8	8 494.380	0.415	0.414	0.001	88.09
	9	9	8 493.791	−0.174	−0.173	−0.000	100.00
$\nu_{central}$: 26 999.4916(17) MHz							
11 2 9 → 11 2 10	10	10	26 999.102	−0.390	−0.389	−0.001	83.89
	11	11	27 000.171	0.679	0.676	0.003	91.25
	12	12	26 999.194	−0.298	−0.295	−0.002	100.00

splittings calculated from the optimized molecular parameters.

$J_{K_a K_c} \rightarrow J'_{K'_a K'_c}$	M'_J	M_J	M_I	$\nu_{obs.}$	$\Delta\nu_{obs.}$	$\Delta\nu_{calc.}$	$\delta\nu$	rel. int./%
$\nu_{central}$: 11 982.2729 MHz								
Magnetic field strength 15 634 G								
1 1 1 → 2 0 2	−1	−2	−1	11 980.718	−1.555	−1.556	0.001	100.00
	−1	−2	0	11 979.356	−2.917	−2.917	0.000	97.19
	−0	−1	−1	11 982.084	−0.189	−0.189	0.000	48.01
	−1	−2	−1	11 980.585	−1.688	−1.688	−0.000	96.62
	0	−1	0	11 983.709	1.436	1.440	−0.004	48.29
	0	1	−1	11 981.326	−0.947	−0.946	−0.001	49.50
	0	−1	1	11 982.038	−0.235	−0.235	0.000	49.52
	0	1	0	11 983.021	0.748	0.744	0.004	47.52
	1	2	−1	11 984.856	2.583	2.582	0.001	95.35
	0	2	1	11 981.264	−1.009	−1.008	−0.001	48.25
	1	2	0	11 983.425	1.152	1.152	0.000	97.51
	1	2	1	11 984.724	2.451	2.452	−0.001	100.00

$J_{K_a K_c} \rightarrow J'_{K'_a K'_c}$	M_J	M_I	$\nu_{obs.}$	$\Delta\nu_{obs.}$	$\Delta\nu_{calc.}$	$\delta\nu$	rel. int./%
$\nu_{central}$: 11 982.2729 MHz							
Magnetic field strength 10 494 G							
1 1 1 → 2 0 2	−1	−1	11 980.767	−1.506	−1.508	0.001	76.44
	−1	0	11 980.282	−1.991	−1.991	−0.000	73.59
	0	−1	11 981.645	−0.628	−0.629	0.000	99.75
	−1	1	11 980.625	−1.648	−1.650	0.001	72.04
	0	0	11 983.543	1.270	1.269	0.001	97.38
	1	−1	11 984.264	1.991	1.990	0.000	70.48
	0	1	11 981.539	−0.734	−0.735	0.001	100.00
	1	0	11 983.768	1.495	1.498	−0.003	74.16
	1	1	11 984.071	1.798	1.800	−0.003	76.84
$\nu_{central}$: 11 982.2729 MHz							
Magnetic field strength 13 081 G							
1 1 1 → 2 0 2	−1	−1	11 980.388	−1.885	−1.884	−0.001	75.97
	−1	0	11 979.917	−2.356	−2.354	−0.002	74.11
	0	−1	11 981.630	−0.643	−0.642	−0.001	99.87
	−1	1	11 980.263	−2.010	−2.009	−0.001	73.01
	0	0	11 983.566	1.293	1.292	0.001	98.25
	1	−1	11 984.610	2.337	2.335	0.002	72.14
	0	1	11 981.545	−0.782	−0.729	0.001	100.00
	1	0	11 984.141	1.868	1.868	−0.001	74.41
	1	1	11 984.465	2.192	2.192	0.000	76.19
$\nu_{central}$: 11 568.0487 MHz							
Magnetic field strength 10 494 G							
3 0 3 → 2 1 2	−2	−1	11 568.924	0.875	0.873	0.002	55.02
	−2	0	11 569.270	1.221	1.219	0.002	53.02
	−1	−1	11 568.760	0.711	0.709	0.002	87.39
	−2	1	11 568.849	0.800	0.799	0.001	53.66
	−1	0	11 568.151	0.102	0.101	0.001	87.19
	0	−1	11 568.388	0.339	0.338	0.001	99.24
	−1	1	11 568.707	0.658	0.657	0.001	87.72
	0	0	11 567.453	−0.596	−0.595	−0.001	100.00
	1	−1	11 567.795	−0.264	−0.253	−0.002	87.84
	0	1	11 568.338	0.289	0.288	0.001	99.28
	1	0	11 567.160	−0.889	−0.889	−0.001	87.52
	2	−1	11 566.987	−1.062	−1.059	−0.003	53.86
	1	1	11 567.738	−0.311	−0.310	−0.001	87.42
	2	0	11 567.261	−0.788	−0.788	0.000	53.67
	2	1	11 566.898	−1.151	−1.148	−0.003	55.38

$J_{K_a K_c} \rightarrow J'_{K'_a K'_c}$	M_J	M_I	$\nu_{obs.}$	$\Delta\nu_{obs.}$	$\Delta\nu_{calc.}$	$\delta\nu$	rel. int./%
$\nu_{central}$: 11 568.0487 MHz							
Magnetic field strength 13 081 G							
3 0 3 → 2 1 2	−2	−1	11 569.139	1.090	1.091	−0.001	55.24
	−2	0	11 569.492	1.443	1.443	−0.001	54.44
	−1	−1	11 568.873	0.824	0.824	0.000	87.92
	−2	1	11 569.082	1.033	1.034	−0.002	54.33
	−1	0	11 568.269	0.220	0.220	−0.000	87.79
	0	−1	11 568.388	0.339	0.338	0.000	99.52
	−1	1	11 568.833	0.784	0.783	0.000	88.17
	0	0	11 567.457	−0.592	−0.591	−0.001	100.00
	1	−1	11 567.673	−0.376	−0.375	−0.001	88.22
	0	1	11 568.348	0.299	0.298	0.001	99.56
	1	0	11 567.047	−1.002	−1.004	0.001	87.99
	2	−1	11 566.735	−1.314	−1.314	−0.000	54.45
	1	1	11 567.626	−0.423	−0.423	−0.000	87.95
	2	0	11 567.027	−1.022	−1.025	0.002	54.35
	2	1	11 566.661	−1.388	−1.389	0.000	55.43
$\nu_{central}$: 10 673.4421 MHz							
Magnetic field strength 17 813 G							
3 1 2 → 3 1 3	−3	−1	10 671.981	−1.461	−1.458	−0.002	100.00
	−3	0	10 673.479	0.037	0.034	0.003	97.77
	−2	−1	10 672.984	−0.458	−0.458	0.001	43.23
	−3	1	10 671.868	−1.574	−1.574	0.000	98.28
	−2	0	10 672.903	−0.539	−0.539	0.000	43.16
	−1	−1	10 673.626	0.184	0.183	0.001	10.87
	−2	1	10 672.755	−0.687	−0.687	0.001	43.72
	−1	0	10 672.624	−0.818	−0.816	−0.001	10.92
	−1	1	10 673.436	−0.006	−0.005	−0.000	10.98
	1	−1	10 674.185	0.743	0.743	0.000	11.00
	1	0	10 673.087	−0.355	−0.354	−0.001	10.95
	2	−1	10 674.127	0.685	0.686	−0.001	43.75
	1	1	10 674.010	0.568	0.569	0.000	10.89
	2	0	10 673.937	0.495	0.500	−0.004	42.86
	3	−1	10 673.803	0.361	0.362	−0.001	97.41
	2	1	10 673.922	0.480	0.485	−0.004	43.62
	3	0	10 673.334	1.892	1.891	0.002	98.56
	3	1	10 673.662	0.220	0.221	−0.001	100.00
$\nu_{central}$: 10 673.4421 MHz							
Magnetic field strength 15 634 G							
3 1 2 → 3 1 3	−3	−1	10 672.107	−1.335	−1.335	−0.000	100.00
	−3	0	10 673.584	0.142	0.141	0.000	97.05
	−2	−1	10 673.071	−0.371	−0.374	0.002	42.84
	−3	1	10 671.977	−1.465	−1.464	−0.002	97.83
	−2	0	10 672.973	−0.469	−0.470	0.000	42.81
	−1	−1	10 673.662	0.220	0.218	0.002	10.79
	−2	1	10 672.808	−0.634	−0.636	0.001	43.51
	−1	0	10 672.654	−0.788	−0.788	−0.000	10.87
	−1	1	10 673.449	0.007	0.003	0.003	10.94
	1	−1	10 674.152	0.710	0.709	0.001	10.97
	1	0	10 673.036	−0.406	−0.407	0.000	10.91
	2	−1	10 674.077	0.635	0.635	−0.000	43.56
	1	1	10 673.953	0.511	0.511	−0.001	10.83
	2	0	10 673.857	0.415	0.420	−0.005	42.39
	3	−1	10 673.744	0.302	0.302	−0.001	96.62
	2	1	10 673.857	0.415	0.407	0.007	43.41
	3	0	10 675.261	1.819	1.817	0.001	98.19
	3	1	10 673.581	0.139	0.139	−0.000	100.00

Table 5. Diagonal elements of the molecular g-tensor and anisotropies in the diagonal elements of the molecular magnetic susceptibility tensor in units of 10^{-6} erg G^{-2} mole^{-1} of formaldoxime.

$\alpha = 2\xi_{aa} - \xi_{bb} - \xi_{cc}$	5.30(11)
$\beta = 2\xi_{bb} - \xi_{aa} - \xi_{cc}$	7.42(06)
g_{aa}	−0.45213(14)
g_{bb}	−0.05270(6)
g_{cc}	−0.01147(6)

Table 6. Correlation coefficient matrix of the least squares fit.

	g_{aa}	g_{bb}	g_{cc}	α	β
g_{aa}	1.000				
g_{bb}	0.867	1.000			
g_{cc}	0.853	0.972	1.000		
α	0.008	0.006	0.006	1.000	
β	−0.007	−0.006	−0.006	−0.824	1.000

Derived Molecular Quantities

a) The Diagonal Elements of the Molecular Electric Quadrupole Moment Tensor

The molecular g-tensor elements and magnetic susceptibility anisotropies can be used to derive the diagonal elements of the molecular electric quadrupole moment tensor with respect to the principal inertia axes system ([21] and (11) through (14) of [16]).

$$Q_{aa} = \frac{|e|}{2}\left\{\sum_n^{\text{nuclei}} Z_n(2a_n^2 - b_n^2 - c_n^2)\,|0\rangle - \langle 0|\sum_j^{\text{electrons}}(2a_j^2 - b_j^2 - c_j^2)\,|0\rangle\right\}$$

$$= -\frac{h\,|e|}{16\pi^2 m_p}\left\{\frac{2g_{aa}}{B_a} - \frac{g_{bb}}{B_b} - \frac{g_{cc}}{B_c}\right\} - \frac{2mc^2}{|e|\,N_A}\{2\xi_{aa} - \xi_{bb} - \xi_{cc}\} \quad (1)$$

(and cyclic permutations). For the definition of the symbols cf. [16].

The molecular quadrupole moments calculated with (1) should come close to the vibronic ground state expectation values (see Chapt. B of [15]). They are of use for comparison with ab initio results and for the theoretical treatment of intermolecular interactions at close range.

b) The Anisotropies in the Second Moments of the Electronic Charge Distribution

From the knowledge of the structure of the nuclear frame it is also possible to obtain experimental values for the anisotropies in the second moments of the electronic charge distribution as given by (see Chapt. A of [15] and (16) of [16])

$$\langle 0|\sum_j^{\text{electrons}}(a_j^2 - b_j^2)\,|0\rangle = \sum_n^{\text{nuclei}} Z_n(a_n^2 - b_n^2) + \frac{h}{8\pi^2 m_p}\left(\frac{g_{aa}}{B_a} - \frac{g_{bb}}{B_b}\right) + \frac{4mc^2}{3e^2 N_A}\{(2\xi_{aa} - \xi_{bb} - \xi_{cc}) - (2\xi_{bb} - \xi_{cc} - \xi_{aa})\} \quad (2)$$

(and cyclic permutations).

This equation is valid in the rigid nuclear frame approximation. Since vibronic ground state expectation values enter for the g-values, rotational constants and susceptibility anisotropies, while r_s-structural data enter for the nuclear configuration, the meaning of the anisotropies determined by (2) is slightly blurred. However, the nuclear second moments which enter into (2) are fairly insensitive with respect to slight changes in the structure. We therefore believe that for them an assumed uncertainty of $0.1 \cdot 10^{-16}\,\text{cm}^2$ is a very conservative estimate and that anisotropies determined from (2) are still meaningful for comparison with quantum chemical results.

We present our molecular electric quadrupole moments and the anisotropies in the second moments of electronic charge distribution in Table 7. Also given for comparison are the corresponding values calculated from Hartree Fock SCF wavefunctions with the "Gaussian 86" progam package [22]. These quantum chemical calculations were carried out at the r_s-structure shown in Figure 1. The standard basis 6-311 G**, i.e. triple zeta with polarization (p-orbitals at H and d-orbitals at C, N, O) was used for this calculation.

c) The Individual Components of the Magnetic Susceptibility Tensor and of the Second Moments of the Electronic Charge Distribution

If the experimental value for the bulk susceptibility were known, which is not the case, also the individual components of the magnetic susceptibility tensor, ξ_{aa}, ξ_{bb}, ξ_{cc}, and the individual second electronic mo-

Table 7. Components of the molecular electric quadrupole moment tensor and anisotropies in the second moments of the electronic charge distribution as calculated from the experimental data. Also given are the corresponding theoretical values. The second moments of the nuclear charge distribution which enter into (2) follow from the r_s-structure shown in Fig. 1 as $\sum_n Z_n a_n^2 = 25.49(25)$ Å^2 and $\sum_n Z_n b_n^2 = 4.74(5)$ Å^2. Given uncertainties are estimated as 1% in order to account for zero point vibrational effects.

	Experimental	TZVP
$Q_{aa}/10^{-26}$ esu cm^2	6.37(8)	6.56
$Q_{bb}/10^{-26}$ esu cm^2	−2.91(6)	−2.91
$Q_{cc}/10^{-26}$ esu cm^2	−3.46(12)	−3.65
$\langle\lvert\sum a_i^2 - b_i^2\rvert\rangle$/Å^2	19.46(32)	19.43
$\langle\lvert\sum b_i^2 - c_i^2\rvert\rangle$/Å^2	4.66(7)	4.64
$\langle\lvert\sum c_i^2 - a_i^2\rvert\rangle$/Å^2	−24.12(28)	−24.07

ments,

$$\langle a^2\rangle = \langle 0|\sum_j^{\text{electrons}} a_j^2\,|0\rangle$$

(and cyclic permutations), could be derived from the experimental data (see Chapt. A of [15]). In the present case we have to go the other way round and we take the ab initio value for $\langle c^2\rangle$ rather than for $\langle a^2\rangle$ or $\langle b^2\rangle$ because this value is least susceptible to uncertainties in the bond distance and bond angles. From the theoretical expressions for the g- and ξ-tensor elements, $\langle c^2\rangle$ is related to those by

$$\langle c^2\rangle = \frac{2mc^2}{e^2 N_A}(\xi_{cc} - \xi_{aa} - \xi_{bb}) + \frac{h}{16\pi^2 m_p}\left(\frac{g_{cc}}{B_c} - \frac{g_{aa}}{B_a} - \frac{g_{bb}}{B_b}\right), \quad (3)$$

Solving (3) for $(\xi_{cc} - \xi_{aa} - \xi_{bb})$ and combining this value with the experimental susceptibility anisotropies from Table 5, it is possible to get the individual susceptibilities as

$$\xi_{aa} = -19.05(84)\cdot 10^{-6}\ \text{erg G}^{-2}\ \text{mole}^{-1},$$
$$\xi_{bb} = -18.35(83)\cdot 10^{-6}\ \text{erg G}^{-2}\ \text{mole}^{-1},$$
$$\xi_{cc} = -25.06(86)\cdot 10^{-6}\ \text{erg G}^{-2}\ \text{mole}^{-1},$$

and the bulk susceptibility as

$$\xi = (\xi_{aa} + \xi_{bb} + \xi_{cc})/3 = -20.82(51)\cdot 10^{-6}\ \text{erg G}^{-2}\ \text{mole}^{-1}.$$

The given uncertainties follow by gaussian error propagation taking into account the experimental uncertainties given in Table 5 and an assumed uncertainty of $0.1\cdot 10^{-16}$ cm^2 in the ab initio value for $\langle c^2\rangle$. We believe that this assumed uncertainty includes also effects of vibrational averaging since the large amplitude out-of-plane OH-torsion only leads to a $0.02\cdot 10^{-16}$ cm^2 increase in $\langle c^2\rangle$. This value was estimated within the harmonic oscillator approximation from its known frequency ($\bar{\nu} = 330$ cm^{-1} [1]) and from a TZVP SCF value for $\langle c^2\rangle$ calculated for a torsional angle of 20° with all other structural parameters fixed to their r_s-values.

Comparison of the Experimental ^{14}N Spin-Rotation Coupling Constants, the ^{14}N Quadrupole Coupling Constants, and the Molecular Electric Quadrupole Moment Tensor with Quantum Chemical Calculations

a) Spin-Rotation Coupling

Spin-rotation coupling arises from the interaction of the nuclear magnetic dipole moment (here the ^{14}N dipole) with the magnetic field caused by the overall rotation of the molecular charge distribution. Since the latter is associated with $\boldsymbol{J}$ while the former is associated with $\boldsymbol{I}$, and since the size of the magnetic field also depends on the orientation of the axis of rotation within the molecule, it may be written phenomenologically (in frequency units) as

$$\hat{\mathcal{H}}_{SR}/h = -\boldsymbol{I}\cdot\mathbf{M}\cdot\boldsymbol{J}, \quad (4)$$

where $\mathbf{M}$ is the spin-rotation coupling tensor. From a detailed theoretical treatment, Flygare [23] has derived the expressions for the $\mathbf{M}$-tensor elements ((6) of [23]). They contain a nuclear contribution which is easily calculated from the known structure, and an electronic contribution which involves a perturbation sum over electronic momentum operators. Within a "localized theory" Flygare also proposed an approximate expression for the latter:

$$M_{aa}^{el} = -\frac{4|e|\,\mu_n\, g_N\, B_a\,\hbar}{cm\,|\Delta E|}\cdot\left\langle\frac{1}{r^3}\right\rangle_p \cdot (P_{bb} + P_{cc} - P_{bb}\cdot P_{cc} + P_{bc}\cdot P_{cb}) \quad (5)$$

(and cyclic permutations), where r stands for the distance of an electron from the nitrogen nucleus, $\langle 1/r^3\rangle_p$ stands for the average value of $1/r^3$ for a p-electron at the nitrogen and P_{aa} etc. are the p-density matrix elements at the nitrogen (compare (5) of [16]). In con-

trast to Flygare we believe that (5) is a reasonable approximation only for the direct local electronic contribution to M_{aa} and that electrons "localized" at the other nuclei should be regarded as compensating the corresponding nuclear contributions. We therefore propose to use (5) directly as an approximate expression for the spin-rotation coupling constants of first row atoms, i.e. we propose to drop the nuclear contribution in Flygare's expression. This approach would be similar to the well known Townes Dailey method (compare [24]) for estimating ^{14}N nuclear quadrupole coupling constants from the p-electron densities at the nitrogen under consideration. (Here the electrons "localized" at the other nuclei are assumed to compensate the corresponding nuclear contributions to the intramolecular field gradient.) It would also agree with the line of thought used in Chapt. 8.-8 of [25] to account for the electronic contribution to the molecular moment of inertia tensor. Finally it would be in agreement with the expermental results of Fabricant, Krieger, and Muenter [26] for proton and deuterium spin-rotation coupling in formaldehyde, thioformaldehyde etc., were quite sizable nuclear contributions (on the order of 100 kHz) are indeed almost compensated or slightly overcompensated by the contributions of "their" electrons, and where no local p-contributions should arise within the revised Flygare model proposed here. CNDO/2- and INDO-p-densities should be sufficient for such an estimate. Our INDO-p-densities, calculated at the r_s-structure are presented in Table 8. The original parametrization of Pople and Beveridge [27] was used in our program. From these p-densities and the n $\rightarrow \pi^*$ excitation energy of 5.6 eV [28], (5) leads to the following values for the local electronic contributions to the spin-rotation coupling constants:

$$M_{aa}^{el} = -0.0184 \text{ MHz},$$
$$M_{bb}^{el} = -0.0033 \text{ MHz},$$
$$M_{cc}^{el} = -0.0029 \text{ MHz}.$$

Table 8. INDO nitrogen p-orbital density matrix elements P_{ij} ($i, j = p_a, p_b, p_c$) of formaldoxime used for the calculation of the spin-rotation coupling constants according to Flygare's approximation.

	p_a	p_b	p_c
p_a	0.9798	−0.1481	0.0000
p_b	−0.1481	1.3852	0.0000
p_c	0.0000	0.0000	1.0669

We note that in spite of the crude approximations which lead to Flygare's local approximation the above values are in amazing agreement with the experimental results.

b) ^{14}N Nuclear Quadrupole Coupling

The experimental nuclear quadrupole constants are related to the vibronic ground state expectation values of the second derivatives of the intramolecular Coulomb potential at the ^{14}N nucleus by

$$\chi_{aa} = \frac{|e|\, Q(\partial^2 V/\partial a^2)}{h} \tag{6}$$

(and cyclic permutation), with e the electronic charge, Q the ^{14}N nuclear quadrupole moment, V the intramolecular Coulomb potential at the nucleus caused by the extranuclear charge distribution, and h Planck's constant.

Within the rigid nuclear frame approximation the electronic ground state expectation values for $(\partial^2 V/\partial a^2)$ etc. are given by

$$\left(\frac{\partial^2 V}{\partial a^2}\right) = \sum_n^{\text{nuclei}} Z_n |e| \frac{3a_{n\text{N}}^2 - r_{n\text{N}}^2}{r_{n\text{N}}^5} - |e| \langle 0| \sum_i^{\text{electrons}} \frac{3a_{i\text{N}}^2 - r_{i\text{N}}^2}{r_{i\text{N}}^5} |0\rangle \tag{7}$$

(and cyclic permutations) with $a_{n\text{N}} = a_n - a_{\text{N}}$ and $a_{i\text{N}} = a_i - a_{\text{N}}$ the a-coordinates of the n-th nucleus and the i-th electron with respect to the nitrogen nucleus, and with $r_{n\text{N}}$ and $r_{i\text{N}}$ the corresponding distances. The "Gaussian 86" program package was used to calculate these expectation values with 6-311 G** Hartree Fock SCF wavefunctions. In order to get a feeling for the vibrational dependence we did not only run the program for the r_s-structure but also for an additional OH-torsional angle $\tau = 20°$ (rather than $\tau = 0°$), for two additional CNO-angles, β, and for a torsional around the C=N double bond. Except for the one angle changed, all other structural parameters were held fixed to their r_s-values. The results are given in Table 9, in which we present the electric field gradients in atomic units rather than the second derivatives of the Coulomb potential. (The latter follow by multiplication with $-|e|/a_0^3$ with a_0 = Bohr's radius.) To convert the field gradients into the experimental quadrupole coupling constants according to (6), the ^{14}N nuclear quadrupole moment Q should be known. Unfortunately its exact value appears to be still unknown. We

Table 9. 6-311G** field gradients at the ^{14}N nucleus (in atomic units) calculated at the r_s-structure (see Fig. 1) for an OH-torsion angle $\tau = 20°$, for extra CNO-angles of 120.2° and 100.2°. In addition, the torsion of the methylen-group was taken into account by carrying out calculations on another two configurations: a 10° torsion of the methylene group combined with a +20° (*a*) and −20° (*b*) torsion of the OH-group, respectively.

	q_{aa}	q_{bb}	q_{cc}
r_s-structure	−0.6945	1.1946	−0.5000
$\tau = 20°$	−0.7007	1.1974	−0.4967
$\beta = 120.2°$	−0.7326	1.3262	−0.5937
$\beta = 100.2°$	−0.6613	1.0657	−0.4044
a	−0.1701	1.1962	−0.4949
b	−0.7021	1.1924	−0.4903

Table 10. ^{14}N nuclear quadrupole coupling constants obtained from the ab initio gradient at the r_s-structure. The conversion factor $-(e^2 \cdot 10^{-33}/a_0^3\ \mathrm{h}) = -0.234973$ MHz a.u.$^{-1}$ mbarn^{-1} was used. The values for the ^{14}N nuclear quadrupole moment were: $Q_1 = 17.4$ mbarn (29), $Q_2 = 19.3$ mbarn (30), $Q_3 = 20.5$ mbarn (31).

	Experimental	Q_1	Q_2	Q_3
χ_{aa}	3.0002(32)	2.8395	3.1495	3.3454
χ_{bb}	−4.6900(20)	−4.8842	−5.4175	−5.7543
χ_{cc}	1.6898(20)	2.0443	2.2675	2.4085

quote three values:

$Q_1 = 17.4(2)$ mbarn [29],

$Q_2 = 19.3(8)$ mbarn [30],

$Q_3 = 20.5(5)$ mbarn [31]

(compare also [7]).

With a conversion factor −0.234973 MHz a.u.$^{-1}$ mbarn^{-1} to convert from the field gradients (in atomic units) and the nuclear quadrupole moment (in mbarn) to the quadrupole coupling constants, the values given in Table 10 are obtained. Clearly the calculated coupling constants differ from the experimental values well outside the quoted uncertainties. Reasons for this discrepancy might be:

a) our neglection of vibrational averaging,
b) our neglection of electron correlation in the ab initio treatment,
c) deficiencies of the basis set.

In view of the fact that the field gradients calculated at different geometries only lead to minor changes (on the order of 0.3% or less if averaged over the corresponding vibration), vibrational influences appear to be of minor importance. Thus, the discrepancies seem to be caused essentially by errors in the electronic expectation value in (7). For each choice of Q these errors may be estimated from the experimental coupling constants and from the nuclear contributions to the second derivatives of the intramolecular Coulomb potential. As it turns out, the ab initio results for the electronic contributions are by 10 to 20% too large (depending on the choice of Q). We note that the necessity for such a systematic downscaling of the electronic contribution to the field gradients calculated by SCF methods was demonstrated recently by Brown and Head-Gordon [32], and we believe that it is mainly caused by the neglect of electron correlation*.

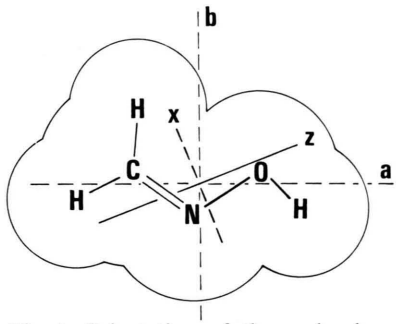

Fig. 4. Orientation of the molecular electric quadrupole moment tensor calculated from the TZVP values of Table 7 and $Q_{ab} = 4.4325 \cdot 10^{-26}$ esu cm^2.

$\theta_{az} = 21.56°$;
$Q_x = -4.6576 \cdot 10^{-26}$ esu cm^2;
$Q_z = 8.3122 \cdot 10^{-26}$ esu cm^2.

θ_{az} denotes the angle between the *a*-axis of the principal inertia axes system and the *z*-axis of the coupling tensor.

c) The Molecular Electric Quadrupole Moments

While the SCF 6-311 G** wavefunctions fail to reproduce the ^{14}N quadrupole coupling constants satisfactorily, they lead to molecular electric quadrupole moments which are in pleasing agreement with the experiment. They are given in Table 7. We are therefore rather confident that the SCF value for the only off-diagonal element of the molecular quadrupole moment tensor is fairly accurate too, and we present the orientation of the tensor in Figure 4.

Acknowledgements

We would like to thank Fonds der Deutschen Chemischen Industrie for financial support and Prof. Dr. A. Guarnieri for critically reading the manuscript. The ab initio calculations were carried out at the CRAY computer of the Rechenzentrum der Universität Kiel.

* Our experimental results for χ_+ and χ_- would be in agreement with $Q(^{14}N) = 17.93$ mbarn and a downsealing of the TZVP result for the electronic contribution to 93% of its value.

[1] I. N. Levine, J. Molec. Spectr. **8,** 276 (1962).
[2] I. N. Levine, Dissertation, Harvard University (1962); Dissertation Abstr. **24,** 1850 (1962).
[3] I. N. Levine, J. Chem. Phys. **38,** 2326 (1963).
[4] M. G. K. Pillai, J. Phys. Chem. **66,** 179 (1962).
[5] V. K. Kaushik and K. Tagaki, J. Phys. Soc. Japan **45,** 1975 (1978).
[6] M. H. Palmer, Z. Naturforsch. **41a,** 147 (1986).
[7] S. Gerber and H. Huber, Chem. Phys. **134,** 279 (1989).
[8] R. Scholl, Berichte **24,** 573 (1891).
[9] B. Kleibömer and D. H. Sutter, Z. Naturforsch. **43a,** 561 (1988).
[10] O. Böttcher, B. Kleibömer, and D. H. Sutter, Ber. Bunsenges. Phys. Chem. **93,** 207 (1989).
[11] W. H. Stolze and D. H. Sutter, Z. Naturforsch. **39a,** 1104 (1984).
[12] O. Böttcher and D. H. Sutter, Z. Naturforsch. **43a,** 47 (1989), Appendix.
[13] I. Merke and H. Dreizler, Z. Naturforsch. **43a,** 196 (1989).
[14] J. Haeckel and H. Mäder, Z. Naturforsch. **43a,** 203 (1988).
[15] D. H. Sutter and W. H. Flygare, Topics in Current Chemistry **63,** 89 (1976).
[16] H. Krause, D. H. Sutter, and M. H. Palmer, Z. Naturforsch. **44a,** 1063 (1989).
[17] H. D. Rudolph, Z. Naturforsch. **23a,** 540 (1968).
[18] W. Gordy and R. L. Cook, Microwave Molecular Spectra, 3rd Edition, Interscience Publishers, New York 1984.
[19] M. Stolze and D. H. Sutter, Z. Naturforsch. **40a,** 998 (1985).
[20] J. Spieckermann and D. H. Sutter, Z. Naturforsch. **44a,** 1087 (1989).
[21] W. Hüttner, M. K. Lo, and W. H. Flygare, J. Chem. Phys. **48,** 1206 (1968).
[22] Gaussian 86, Carnegie-Mellon Quantum Chemistry Publishing Unit, Pittsburg PA 1984.
[23] W. H. Flygare, J. Chem. Phys. **41,** 793 (1964).
[24] J. Mjöberg and S. Ljungren, Z. Naturforsch. **28a,** 729 (1973).
[25] C. H. Townes and A. L. Schawlow, Microwave Spectroscopy, Dover Publications, New York 1975.
[26] B. Fabricant, D. Krieger, and J. S. Muenter, J. Chem. Phy. **67,** 1576 (1977).
[27] J. A. Pople and D. L. Beveridge, Approximate Molecular Orbital Theory, McGraw Hill Book Company, New York 1979.
[28] R. Ditchfield, J. E. Del Bene, and J. A. Pople, J. Amer. Chem. Soc. **94,** 703 (1972).
[29] N. Ensllin, W. Bertozzi, S. Kowalski, C. P. Sargent, W. Turchinetz, C. F. Williamson, S. P. Fivozinsky, J. W. Lightbody, and S. Penner, Phys. Rev. (C) **9,** 1705 (1974).
[30] H. Winter and H. J. Andrä, Phys. Rev. (A) **21,** 581 (1980).
[31] D. Sundholm, P. Pyykkö, L. Laaksonen, and A. J. Sadley, Chem. Phys. **101,** 219 (1986).
[32] R. D. Brown and M. P. Head-Gordon, Mol. Phys. **61,** 1183 (1987).
[33] H. Dreizler, Mol. Phys. **59,** 1 (1986).